Optimal control model for the critical state in superconductors

A. Badía*
Física de la Materia Condensada, C.P.S.I. Universidad de Zaragoza, María de Luna 3, E-50.015 Zaragoza, Spain

C. López
Matemática Aplicada, C.P.S.I. Universidad de Zaragoza, María de Luna 3, E-50.015 Zaragoza, Spain

J. L. Giordano
Ciencia y Tecnología de Materiales y Fluidos, C.P.S.I. Universidad de Zaragoza, María de Luna 3, E-50.015 Zaragoza, Spain
(Received 14 May 1998)

Grounded on a variational principle, we present a generalization of the standard critical-state approach in type-II superconductors. The free energy is minimized with the constraint $|\mathbf{J}(\mathbf{r})| \leqslant J_c$ for the macroscopic current density, posing the problem in the framework of the optimal control theory. The application of this mathematical tool allows us to determine the critical state in which the system organizes itself. This permits to confirm the critical-state hypothesis for an idealized one-dimensional geometry and to deal with multicomponent field situations, for which additional constitutive laws are provided. A geometrical picture of the field penetration process has been developed and we obtain both analytical and numerical solutions for two-dimensional problems under an applied parallel field and superimposed transport current.
[S0163-1829(98)06038-X]

I. INTRODUCTION

Variational calculus is a basic mathematical tool used in fundamental physical theories and has had a most successful application throughout basic sciences and engineering. In its most simple formulation it solves the problem of looking for paths which are stationary for an integral functional depending on position and velocity, and giving as necessary conditions the well-known Euler-Lagrange equations. Its formulation in terms of Hamilton equations is a cornerstone of quantum mechanics, and has also provided a framework for problems with constraints.

A generalization of variational calculus, the optimal control (OC) theory, has been developed since the seminal work by Pontryagin *et al.*[1] For a more comprehensive review, the interested reader is directed to see, for instance, Refs. 2 and 3. In this formulation, some control variables $\mathbf{u}$ drive the evolution of the state variables $\mathbf{x}$ through a differential equation $\dot{\mathbf{x}}=\mathbf{f}(\mathbf{x},\mathbf{u})$, while some cost or objective functional $\int \mathcal{L}(\mathbf{x},\mathbf{u})dt$ must be minimized. Considering $\dot{\mathbf{x}}=\mathbf{u}$ one reproduces the classical variational problem as a particular case of OC theory. Moreover, the Pontryagin maximum principle allows us to consider constraints of the type $g_\alpha(\mathbf{u}) \leqslant c_\alpha$ (spaces with boundaries), so that closed as well as open sets can be managed. This powerful generalization of variational calculus has been successfully used in a broad range of fields, including pure and applied mathematics (Finsler[4,5] or sub-Riemannian geometry,[6,7] applications to engineering, economics, etc.). Nevertheless, to our knowledge, fundamental and applied physics are scarcely touched areas by OC theory. We believe that, most probably, there are a number of physical phenomena for which heuristic approximations can be made in terms of inequality-constrained control-like variables. In this article, we propose an optimal control model to solve some open questions on the behavior of superconducting materials.

Recall that a superconductor bears the property of developing nondissipative currents which try to expel any applied magnetic field.[8] This behavior can be recorded in macroscopic experiments, which are sensitive to thermodynamic averages over the sample's volume. In particular, it is a common practice to characterize the magnetostatics of the specimen by means of a magnetization curve $\vec{\mathfrak{M}}(\vec{\mathfrak{H}})$. Here, $\vec{\mathfrak{M}}$ represents the sample's magnetic moment per unit volume and $\vec{\mathfrak{H}}$ is the magnetic field vector related to the controllable sources, which are assumed to be unaffected by the presence of the superconductor.

For the case of type-II superconductors in the vortex state, the full description of the underlying phenomena on which the macroscopic properties rely is highly involved.[9] Nevertheless, many experimental facts can be explained by means of phenomenological models which override the great mathematical difficulties of fundamental theories. This is the case of the *critical-state model* (CSM),[10] which describes the magnetization hysteresis $\mathfrak{M}(\mathfrak{H})$ for strongly pinned (hard) type-II superconductors, without specifying the microscopic mechanism which controls the vortex pinning. The model postulates that the sample holds a steepest metastable gradient of H supported by the underlying pinning force. This is formulated *via* the *critical-state equation* $\nabla \times \mathbf{H} = \mathbf{J}_c$ (or 0). The critical current vector $\mathbf{J}_c$ is related to the pinning properties of the superconductor, typically in the form $|\mathbf{J}_c| = J_c(\mathbf{H})$. Then, the penetration profile $\mathbf{H}(\mathbf{r})$ can be derived when the appropriate boundary conditions are imposed, and this allows us to calculate $\mathfrak{M}$.

The former critical-state equation is readily applicable when there is a unique, known in advance, direction for the current. Nevertheless, this situation is mostly restricted to

idealized (one-dimensional) geometry, whereas the constitutive equation $|\mathbf{J}|=J_c$ (or 0) is not enough to solve the seemingly simple situation in which an external field is applied parallel to the conductive longitudinal current in an infinite cylindrical specimen. Thus, multicomponent problems require additional hypotheses. Several authors[11–13] have proposed a dynamical approach in which Maxwell laws for time-dependent electric and magnetic fields are included. In this paper, we introduce a different method which allows us to obtain the metastable field penetration profile by means of a minimum principle, and includes as a particular case the standard single-component CSM.

The article is organized as follows. In Sec. II we present the general concepts of magnetostatics in terms of which the problem is posed and introduce the variational principle, which together with the notion of the critical current density gives place to a typical optimal control problem. In Sec. III the optimal control machinery is applied to the case of an infinite superconducting slab under the simultaneous action of an external applied field and transport current. Both analytical and numerical solutions are found and discussed in terms of a metric space formulation (taking advantage of a quite general link between optimal control and metric spaces). Section IV displays the resolution for the case of cylindrical symmetry, more awkward to handle, but with obvious interest for experimental situations. A global discussion of our results and some concluding remarks are finally presented in Sec. V.

II. MACROSCOPIC FIELD EQUATIONS: THE VARIATIONAL PRINCIPLE

A typical approach for calculating the magnetostatic response of a superconducting sample to the applied magnetic field $\vec{\mathfrak{M}}(\vec{\mathfrak{H}})$ consists of starting with $\vec{\mathfrak{M}}=\vec{\mathfrak{B}}/\mu_0-\vec{\mathfrak{H}}$ where the specimen's magnetic flux density $\vec{\mathfrak{B}}$ is introduced. This vector is computed in terms of the coarse-grained mean value $\mathbf{B}(\mathbf{r})$:

$$\vec{\mathfrak{B}}=\frac{1}{V}\int_V \mathbf{B}\, d^3\mathbf{r},$$

where integration is extended over the sample's volume. Then, one must supply a sufficient number of relations between the macroscopic fields $\mathbf{B}$, $\mathbf{H}$, and $\mathbf{J}$ if their spatial dependence is to be determined. Ampère's law, together with the appropriate constitutive equations, provides such relations.

For the case of type-I superconductors in the absence of demagnetizing effects, coarse graining is superfluous because current loops only exist at the macroscopic level and $\mathbf{B}=\mu_0\mathbf{H}$ holds. Combining this with Ampère's law $\nabla\times\mathbf{H}=\mathbf{J}$ and the London equation $\mathbf{A}=-(\mu_0\lambda^2)\mathbf{J}$ one can derive the field spatial dependence.

A very useful interpretation of the London equation is that upon standard variation with respect to the vector potential $\mathbf{A}(\mathbf{r})$ of the free energy

$$\mathcal{G}=\frac{1}{2}\int_V(\mu_0\mathbf{H}^2-\mathbf{J}\cdot\mathbf{A})d^3\mathbf{r}, \tag{2.1}$$

one can obtain it as the *Euler-Lagrange* equation of the system. Notice that the minimization of $\mathcal{G}$ can be interpreted as the balance between the decrease of the potential energy associated to the external field pressure and the increase of the kinetic energy related to the superconducting currents.

On the other hand, a much more complex scenario arises for type-II superconductors. For a wide range of external conditions (when H lies between the so-called lower, H_{c1}, and upper, H_{c2}, critical fields), these materials develop an intricate structure (the vortex state) in which they share macroscopic shielding currents and a lattice of quantized flux lines, $\mathbf{\Phi}_0$, each supported by a supercurrent vortex. Thus, one must distinguish between the *microscopic* flux line fluctuating field $\mathbf{b}$ and the *macroscopic* averages, extended over volumes which contain enough number of vortices: $\mathbf{B}\equiv\langle\mathbf{b}\rangle$. Notice that in the context of pinned vortices in type-II superconductors, Ampère's law relates the field $\mathbf{H}$ with the externally imposed macroscopic currents $\mathbf{J}$, while the equilibrium response of the superconductor is described by means of the $\mathbf{B}(\mathbf{H})$ relation.

In the spirit of the CSM, let us now consider a type-II superconductor well apart from the lower and upper critical fields $H_{c1}\ll H\ll H_{c2}$, where $\mathbf{B}=\mu_0\mathbf{H}$ is a good approximation for hard superconductors. In other words, the equilibrium response is neglected respect to the interaction of vortex lines with sample inhomogeneities (pinning centers). We want to get a proper expression for the free energy to be minimized, which will produce the pending constitutive equation. Using n_{L} for the number of flux lines per unit area, the restriction on the field values means that[8] $1/\lambda^2\ll n_{\mathrm{L}}\ll 1/\xi^2$, where λ is the London depth and ξ is the size of the normal core associated with the flux line. Then, one can use the coarse-grained description of the nonoverlapping vortex system and neglect the London kinetic energy of the currents, so that, adopting the *force balance* picture between the magnetostatic stress and the pinning force, and using Ampère's law, we have the averaged relationship

$$\begin{aligned}\mu_0\mathbf{J}\times\mathbf{H}&=\mu_0(\nabla\times\mathbf{H})\times\mathbf{H}\\&=-\frac{\mu_0}{2}\nabla(\mathbf{H}^2)+\mu_0(\mathbf{H}\cdot\nabla)\mathbf{H}\\&=\mathbf{F}_{\mathrm{pinning}},\end{aligned}$$

where $\mathbf{F}_{\mathrm{pinning}}$ denotes the pinning force per unit volume and $F_{p,\max}$ is its maximum absolute value. Then, a metastable equilibrium will be attained when the Lorentz and the pinning forces equal each other. The associated free energy of the flux line lattice in the penetrated sample is therefore

$$\mathcal{G}=\frac{\mu_0}{2}\int_V\mathbf{H}^2d^3\mathbf{r}.$$

However, the induced current distribution which must minimize this energy is subjected to physical limitations. On the one hand, the component of $\mathbf{J}$ perpendicular to $\mathbf{B}$ is constrained by the maximum pinning force to the critical value $J_{c\perp}=F_{p,\max}/B$.[8] In fact, this is the only component which arises in the so-called idealized geometries (infinite slab or cylinder under a parallel field). On the other hand, a critical value $J_{c\|}$ arises associated with flux line cutting

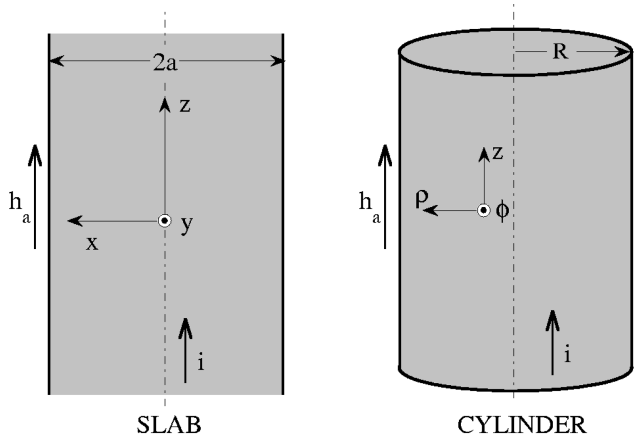

FIG. 1. Sketch of the geometrical configurations studied in this work. Either an infinite superconducting slab or cylinder will be considered, subjected to an applied parallel field h_a and transport current i.

phenomena.[11] If higher currents are demanded, energy losses appear, breaking the superconducting state down. In this work we take the simplifying hypothesis $|\mathbf{J}| \leqslant J_c$ in order to bring out the physics with the least mathematical complication. It is remarkable that such a kind of *isotropic model* has allowed the interpretation of polarized neutron visualization experiments of the magnetic field penetration in high-T_c superconductors.[14] Nevertheless, our approach is valid for any dependence $\mathbf{J}_c(\mathbf{B})$, in particular for the rectangular model:[11] $J_\perp \leqslant J_{c\perp}(\mathbf{B})$, $J_\parallel \leqslant J_{c\parallel}(\mathbf{B})$.

Thus, we propose the following principle for determining the response of a type-II superconductor to an applied magnetic field in the presence of pinning: *In type-II superconductors, the penetration profile of increasing magnetic fields in a virgin sample, fulfilling Ampère's law* $\nabla \times \mathbf{H} = \mathbf{J}$ *and the constraint* $|\mathbf{J}| \leqslant J_c$ *minimizes the magnetostatic energy* $(\mu_0/2)\int_V \mathbf{H}^2 d^3\mathbf{r}$.

The next section is devoted to state the problem within the framework of the OC theory.

III. OPTIMAL CONTROL APPROACH AND ASSOCIATED METRIC

In this section, we briefly illustrate the OC machinery through the particular problem of the slab geometry. Its simplicity allows alternative representations which will lead to a deeper insight into the CSM. One can translate it into a metric problem in the state variables space; one can find analytical solutions for the penetrating fields and a relatively simple numerical integration scheme is originated.

A. Hamiltonian formalism

In order to see how the OC formulation arises, consider a sample with slab geometry (an infinite plane slice with finite depth $2a$) in a parallel field and current configuration (see Fig. 1). $\mathfrak{H}$ will be used for the uniform applied field and $\mathfrak{I}$ for the transport current per unit length, $\mathfrak{I} = 2\int_0^a J_z dx$. We take the origin of coordinates at the center of the slab and the x axis orthogonal to the surface. By virtue of the problem's symmetry the subsequent discussion is restricted to the half space $x \geqslant 0$.

First of all, and for simplicity, let us introduce dimensionless quantities and reduced variables in which the problem will be stated. The sample's half width a will provide the length scale, so that $x = 1$ is the surface coordinate. Additionally, let us denote by H^* the value of the uniform external field $\mathfrak{H}$ in the absence of transport current at which the penetration profile reaches the center of the slab (which coincides with the value of the induced field on the surface of the slab created by the maximal current with no resistive losses). Then, we define $\mathbf{h} \equiv \mathbf{H}/H^*$ and $\mathbf{u}$ a vector perpendicular to $\mathbf{J}$ of magnitude J/J_c. Finally, the dimensionless external field values are indicated by $h_a = \mathfrak{H}/H^*$ and $i = \mathfrak{I}/H^*$.

In terms of the former variables, the problem can be posed as follows: We want to find the field penetration profile $\{\mathbf{h}(x), 0 \leqslant x \leqslant 1\}$ under the following conditions.

(i) The *state equations* (Ampère's law) are

$$\frac{d\mathbf{h}}{dx} = \mathbf{u},$$

(ii) with *state variables* (magnetic field) subjected to the *boundary conditions*

$$h_y(1) = i/2,\ h_z(1) = h_a,\ h_y(0) = 0,$$

because surface currents producing discontinuity in the magnetic field are discarded.

(iii) We require the minimization of the *cost function* (free energy)

$$C[\mathbf{h}(x)] = \int_0^1 \mathbf{h}^2 dx = \int_0^1 \mathcal{L} dx,$$

(iv) with the constraint for the *control variables* (current vector)

$$\mathbf{u} \in \Omega$$

$$\Omega = \{\mathbf{u}(x) : |\mathbf{u}(x)| \leqslant 1\}.$$

The Pontryagin maximum principle gives the solution of the problem. The first step is to define the Hamiltonian associated with the OC problem, introducing the momenta variables $\mathbf{p}$ (Lagrange multipliers):

$$\mathcal{H} = \mathbf{p} \cdot \frac{d\mathbf{h}}{dx} + p_0 \mathcal{L} = \mathbf{p} \cdot \mathbf{u} + p_0 \mathbf{h}^2.$$

Hamilton equations reproduce the state equations and define linear differential equations for the momenta:

$$\frac{d\mathbf{h}}{dx} = \frac{\partial \mathcal{H}}{\partial \mathbf{p}} = \mathbf{u},$$

$$\frac{d\mathbf{p}}{dx} = -\frac{\partial \mathcal{H}}{\partial \mathbf{h}} = -2p_0\mathbf{h}.$$

Additionally, we introduce the equations for defining the *cost variable* s,

$$\frac{ds}{dx} = \frac{\partial \mathcal{H}}{\partial p_0} = \mathbf{h}^2,$$

with the associated equation for p_0:

$$\frac{dp_0}{dx} = -\frac{\partial \mathcal{H}}{\partial s} = 0.$$

The constant p_0 is taken to be negative (or zero, for singular solutions, which is not the case here) and it can be fixed to -1 by rescaling all the momenta (due to the linearity of $\mathcal{H}$ on $\mathbf{p}$).

Now, the theorem states that for the optimal solution of the problem [i.e., functions $\mathbf{h}_c(x)$ and $\mathbf{u}_c(x)$ such that the state equations and boundary conditions are satisfied and C is minimum], it is necessary that momenta functions $\mathbf{p}_c(x)$ exist, satisfying Hamilton equations, and that at every fixed x, the Hamiltonian takes its maximum on the control variables $\mathbf{u}_c$:

$$\mathcal{H}(\mathbf{h}_c, \mathbf{p}_c, \mathbf{u}_c) = \max_{\mathbf{u} \in \Omega} \mathcal{H}(\mathbf{h}_c, \mathbf{p}_c, \mathbf{u}).$$

In our Hamiltonian, the application of this theorem leads to maximizing the term $\mathbf{p} \cdot \mathbf{u}$ on the control space Ω. By virtue of linearity, the solution is $\mathbf{u}_c = \mathbf{p}_c / |\mathbf{p}_c|$ (this means $|\mathbf{J}| = J_c$ and gives the distribution rule for the components of $\mathbf{J}$). We want to stress that, as a major result of this work, criticality is obtained as a necessary condition in the minimization process and not imposed *ab initio* like in the standard CSM approach and, what is more, we have derived the distribution rule from a very fundamental principle.

A direct substitution of the criticality condition ($\mathbf{u}_c = \mathbf{p}_c / |\mathbf{p}_c|$) in the Hamiltonian equations gives as a result

$$\frac{d\mathbf{h}}{dx} = \frac{\mathbf{p}}{|\mathbf{p}|}, \quad \frac{d\mathbf{p}}{dx} = 2\mathbf{h}. \tag{3.1}$$

Notice that, though dealing with the optimal variables, we have dropped the suffix c, just for the sake of brevity.

Four independent boundary conditions are required to determine the integral curves $\mathbf{h}(x), \mathbf{p}(x)$. The set will be formed by means of the physical restrictions on the field values at the boundaries. Accidentally, they will have to be supplemented by the so-called *transversality conditions* applied to the momenta when necessary.

Subsequently, we present several approaches for solving Eqs. (3.1).

B. Analytical solution

Implicit forms of the canonical equation integral curves can be derived by means of the polar coordinate representation. On using the state and control coordinates,

$$\mathbf{h} \equiv (h, \theta) = (|\mathbf{h}|, \arctan(h_z / h_y)),$$

$$\mathbf{u} \equiv (u_h, u_\theta) = (\mathbf{j} \cdot \hat{\boldsymbol{\theta}}, -\mathbf{j} \cdot \hat{\mathbf{h}}),$$

the optimal control Hamiltonian reads

$$\mathcal{H} = -h^2 + p_h u_h + p_\theta u_\theta / h,$$

where $u_h^2 + u_\theta^2 \leqslant 1$.

On the other hand, by applying the maximum principle we get

$$(u_h, u_\theta) = (h p_h, p_\theta) / \sqrt{h^2 p_h^2 + p_\theta^2}.$$

Now, the canonical equations become

$$\frac{dh}{dx} = h p_h / p, \tag{3.2a}$$

$$h \frac{d\theta}{dx} = p_\theta / p, \tag{3.2b}$$

$$\frac{dp_h}{dx} = 2h + p_\theta^2 / (p h^2), \tag{3.2c}$$

$$\frac{dp_\theta}{dx} = 0, \tag{3.2d}$$

with $p = \sqrt{h^2 p_h^2 + p_\theta^2}$.

Next, we will show that one can reduce the problem to quadrature integration when the *constants of the motion* are considered. Observing that the system is autonomous we get the first constant $K \equiv \mathcal{H}$. On the other hand, Eq. (3.2d) shows that the θ component of the momentum is also a conserved quantity, $d \equiv p_\theta$. Then, the penetration profile can be obtained by integration of the following pair of uncoupled differential equations:

$$\frac{dh}{dx} = \frac{\sqrt{(h^2 + K)^2 h^2 - d^2}}{h(h^2 + K)}, \tag{3.3a}$$

$$\frac{d\theta / dx}{dh / dx} = \frac{d\theta}{dh} = \frac{d}{h\sqrt{(h^2 + K)^2 h^2 - d^2}}. \tag{3.3b}$$

In fact, one can classify the integral curves in terms of the constants of motion, which have a close relation with the physical response of the superconductor.

1. Partial penetration ($d = 0$)

A simple solution arises for Eqs. (3.3) when one considers $d = 0$. First of all, we will show that $d = 0 \Rightarrow K = 0$. Indeed, $d = 0$ implies that the magnetic field penetrates parallel to its surface value (as $d\theta / dx = 0$). On the other hand, owing to the topological condition $h_y(0) = 0$, a constant value of θ precludes a nonvanishing magnetic field at the center of the sample [unless for the trivial case $h_y(1) = 0$]. Thus, $d = 0$ is equivalent to the so-called *partial penetration* regime in which both components of $\mathbf{h}$ vanish at some point x_c, being $0 \leqslant x_c < 1$. Furthermore, one can prove that a free final parameter x_c implies $\mathcal{H}(x_c) = 0$ and this means $K = 0$.

Now, the system (3.3) becomes

$$\frac{dh}{dx} = 1, \quad \frac{d\theta}{dx} = 0. \tag{3.4}$$

Thus, $d = 0$ represents the family of penetration profiles for which the magnetic field vector reduces its magnitude linearly towards the slab center, while keeping a constant value h_z / h_y. Taking into account the boundary conditions $h_y(1) = i/2$, $h_z(1) = h_a$, $h_y(x_c) = h_z(x_c) = 0$ one obtains

$$\mathbf{h}(x)=\begin{cases}\mathbf{h}(1)\left(\dfrac{x-x_c}{1-x_c}\right), & x_c\leqslant x\leqslant 1,\\ 0, & 0\leqslant x\leqslant x_c,\end{cases} \tag{3.5}$$

where $x_c=1-\sqrt{h_a^2+(i/2)^2}$ determines the penetration depth of the fields. Therefore, the unit disk on the **h** plane is the set of values at the surface corresponding to partial penetration.

2. *Full penetration* ($d\neq 0$)

Above, we have obtained the partial penetration minimum energy solutions corresponding to $d=0$. In fact, one can easily show that partial penetration only occurs in such a case. Observing Eqs. (3.4) and the cost function, it is apparent that for a given value of x_c, their linear solution holds the lowest possible energy, because h decreases with the maximum slope all around. Thus, $d\neq 0$ corresponds to the family of solutions for which **h** does not vanish at the sample center, $\mathbf{h}(0)\neq 0$ (*full penetration*). Though more intricate, one can still find an analytical representation.

Indefinite integrals of Eqs. (3.3a) and (3.3b) can be expressed in terms of elliptic and associated functions. They admit a simplest representation when reduced to Weierstrass' normal form,[15] i.e.,

$$I=\int \frac{S(z)}{\sqrt{4z^3-g_2z-g_3}}dz,$$

where $S(z)$ means a rational function of z. This can be accomplished with the substitution $h^2=\sqrt[3]{4}\,z-2K/3$ and we get $g_2=(\sqrt[3]{4}/3)K^2$, $g_3=(d^2+2K^3/27)$.

A new change of variable allows us to compute the integral in terms of Weierstrass' $\wp$ function. On using

$$w=\int_z^\infty \frac{dz}{\sqrt{4z^3-g_2z-g_3}}$$

and the inverse relation $z=\wp(w;g_2,g_3)$, we get

$$I=\int S[\wp(w)]dw.$$

Expanding $S[\wp(w)]$ in the form

$$S[\wp(w)]=c_0+c_1\wp(w)+c_2\wp^2(w)+\cdots + \frac{A_1}{\wp(w)-\alpha}+\frac{A_2}{[\wp(w)-\alpha]^2}+\cdots + \frac{B_1}{\wp(w)-\beta}+\cdots,$$

our integrals can be readily evaluated, and we finally come to the implicit solutions

$$x=\sqrt[3]{2}\,\zeta(w)-\frac{K}{3\sqrt[3]{2}}w+C_1,$$

$$\theta=\frac{d}{2\wp'(\alpha)}\left[\log\frac{\sigma(w-\alpha)}{\sigma(w+\alpha)}+2w\zeta(\alpha)\right]+C_2, \tag{3.6}$$

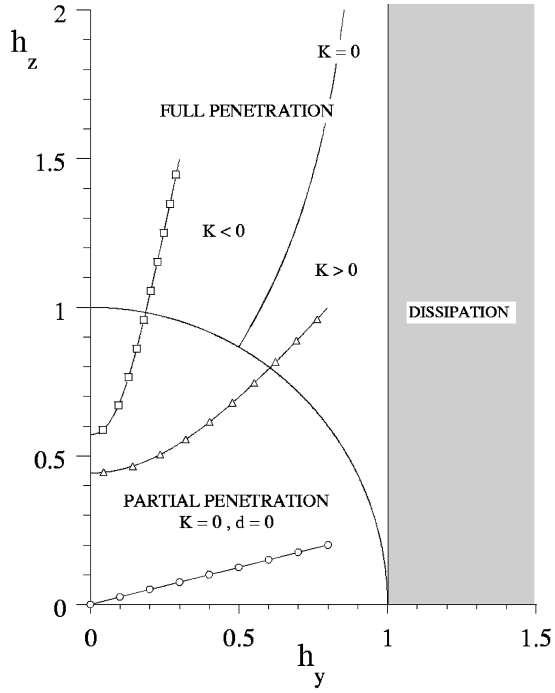

FIG. 2. **h** plane phase diagram representation of the penetration profile in a superconducting slab. The maximum principle Hamiltonian constants of the motion (K,d) are used to classify the solutions in terms of the region where the surface values $h_y(1),h_z(1)$ lie. Typical examples of the profiles for each region are given. The line $K=0$ has been evaluated according to Eqs. (3.7) and approaches the line $h_y=1$ asymptotically. Also outlined is the fact that, owing to resistive losses, superconductivity disappears within the half space $h_y(1)>1$. **H** has been normalized with respect to the penetration field $\mathbf{h}\equiv\mathbf{H}/H^*$.

where α is defined by $\wp(\alpha)=\sqrt[3]{2}K/3$ and we have introduced Weierstrass' ζ and σ functions.

These implicit equations hold for penetration profiles corresponding to surface values on the band $h_y\leqslant 1$ and include, as a particular degenerate case, the partial penetration regime obtained before.

In order to specify the full penetration solutions, the following boundary conditions must be used: $h_1\equiv h(1)=\sqrt{h_a^2+(i/2)^2}$, $\theta_1\equiv\theta(1)=\arctan(2h_a/i)$, $\theta_0\equiv\theta(0)=\pi/2$, and $p_h(0)=0$. Notice that $p_h(0)=0$ has been incorporated, corresponding to the transversality condition related to the arbitrariness in the value of $h_z(0)$.

The curves with starting points on the region $d\neq 0$ can be still further classified in terms of the values of the constant K. In fact, one can produce a quite meaningful *phase diagram* in the **h** plane, dividing it up into several regions (see Fig. 2). The characteristics of the penetration profile are determined by the region on which the initial point $[h_y(1),h_z(1)]$ lies. Archetypical penetration profiles $h_z(h_y)$ are displayed in the same figure.

We want to mention that the points $[h_y(1),h_z(1)]$ for which the penetration profile evolves under the condition $K=0$ univocally determine the line labeled according to that condition. Indeed, $K=0$, $d\neq 0$ leads to the so-called *equianharmonic case* ($g_2=0$, $g_3=1$). Then, definite integration of Eqs. (3.3) gives

$$3\theta_1 = 2\pi - \arcsin(h_0^3/h_1^3),$$

$$\frac{1}{\sqrt[3]{2}} = \zeta(w_1) - \zeta(w_0), \tag{3.7}$$

where the subscripts indicate the point ($x=0,1$) at which the function must be evaluated.

Owing to the multivalued nature of the involved functions, one must be careful when managing Eqs. (3.7). Our expressions assume that the principal values are considered. Notice that for penetration profiles starting at this line, the end point is easily computed: $h_0 = h_1[\sin(2\pi - 3\theta_1)]^{1/3}$.

By virtue of continuity, $K=0$, $d\neq 0$ acts as the separatrix between two regions: (i) $K>0$ corresponds to the region of full penetration where transport currents predominate. (ii) $K<0$ defines the region of full penetration where the external magnetic field predominates.

The penetration profiles and the corresponding currents for the previously presented initial conditions in the different regions of the phase diagram are shown in Fig. 3. Observe that, related to the transversality condition in the minimization process, the shielding component of the current becomes zero at the center, whereas the transport component tends to the maximum value.

C. Associated metric

Again, we will refer to the **h** plane where the parametrized curves $[h_y(x), h_z(x)]$ lie. In fact, a metric structure can be defined on it, whose geodesics are solution curves of the OC problem. This is a particular case of a quite general relationship between OC problems and metric spaces (usually Finslerian). In our case, the associated metric can be easily obtained as follows. First of all, from the state equations $d\mathbf{h}/dx = \mathbf{u}$ and the obtained optimality condition $\mathbf{u}^2 = 1$, it is apparent that the curves $(h_y(x), h_z(x))$ corresponding to penetration profiles of the magnetic field must have Euclidean length less (partial penetration) or equal (full penetration) to 1. Now, the cost variable s, defined by $ds/dx = h^2$, can be used for a reparametrization of the state equations

$$\frac{d\mathbf{h}}{ds} = \frac{d\mathbf{h}\,dx}{dx\,ds} = \frac{\mathbf{u}}{h^2},$$

which, together with the condition $\mathbf{u}^2 = 1$ gives as infinitesimal cost $ds = \sqrt{h^4 (d\mathbf{h})^2}$. This means that the metric $(ds)^2 = h^4 (d\mathbf{h})^2$ can be used to obtain the curves on the **h** plane of minimal s length, i.e., optimal.

The particular metric problem to be solved depends again on the initial values $\mathbf{h}(1)$. For the partial penetration regime $h(1) \leqslant 1$ we must find the geodesic curve of $(ds)^2$ joining this point to the origin $\mathbf{h}(x_c) = 0$. In this case, the geodesics of $(ds)^2$ are straight lines joining the initial point to the origin of the **h** plane, corresponding to the linear solution as shown before [Eq. (3.5)].

For $\mathbf{h}(1)$ lying on the band $h_y(1) \leqslant 1$, $\mathbf{h}^2 > 1$, we must find the curve of minimal s length among those which connect the initial point to the vertical axis $h_y = 0$ with Euclidean length 1 (fixed final parameter $x_c = 0$). This is a typical *isoperimetric* problem, whose solution can be accomplished by

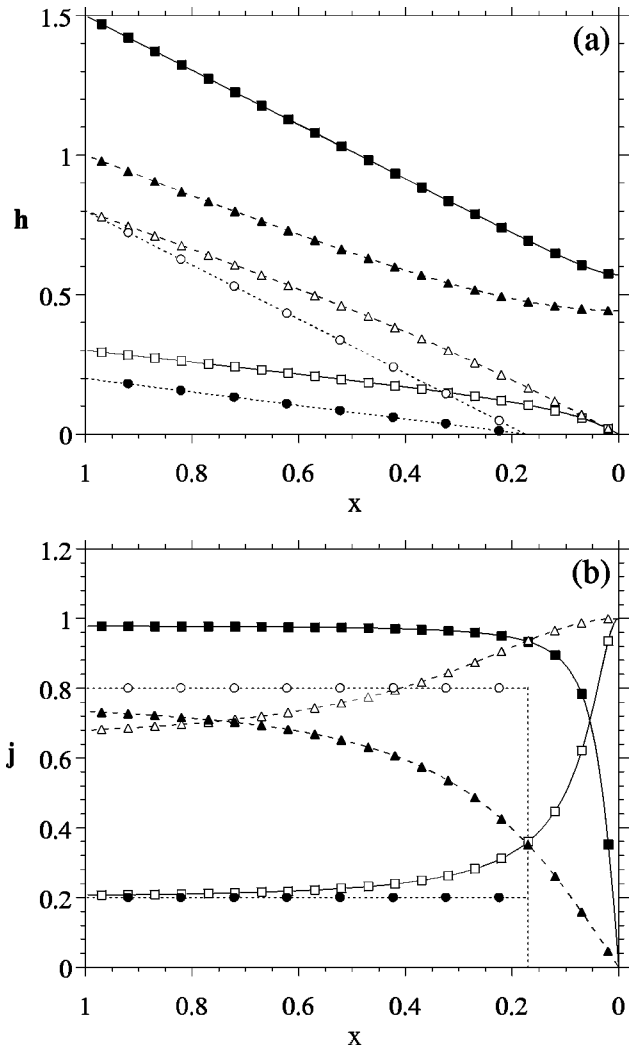

FIG. 3. Magnetic field and current penetration profiles in a superconducting slab for different external conditions $[h_y(1), h_z(1)]$, corresponding to the **h**-plane curves in Fig. 2. Panel (a) displays the reduction of the magnetic field components towards the center of the slab $x=0$. Solid symbols stand for h_z while open symbols represent h_y. Each case is depicted by a symbol type: squares for $\mathbf{h}(1) = (0.3, 1.5)$, triangles for (0.8,1), and circles for (0.8,0.2). Panel (b) displays the associated current profiles. The same symbol convention as in part (a) has been used, whereas solid symbols represent $-j_y$ and open symbols j_z (the minus sign election is for the sake of clarity of the plot). The normalization $\mathbf{h} \equiv \mathbf{H}/H^*$, $\mathbf{j} \equiv \mathbf{J}/J_c$ is used.

obtaining the geodesics of the metric $(ds_\lambda)^2 = (h^2 + \lambda)^2 (d\mathbf{h})^2$, where λ is a constant (Lagrange multiplier) to be determined. Again, by virtue of transversality properties, the geodesic will always intersect the z axis perpendicularly. In this metric language it is again clear that points outside the band (region of resistive losses) cannot be joined to the vertical axis by curves of euclidean length less or equal to 1. Now, it is a simple exercise to obtain the geodesic (Euler-Lagrange) equations for the metric $(ds_\lambda)^2$. On using polar coordinates and parametrizing the curves with the angle variable (invariance under reparametrization holds) we get the Lagrangian

$$\mathcal{L} = (h^2 + \lambda)\sqrt{v_h^2 + h^2},$$

where $v_h = dh/d\theta$. Note that its associated energy is a constant,

$$\mathcal{E} = v_h \frac{\partial \mathcal{L}}{\partial v_h} - \mathcal{L} = -\frac{(h^2+\lambda)h^2}{\sqrt{v_h^2+h^2}} = E_0,$$

from which we obtain the differential equation

$$\frac{dh}{d\theta} = -\frac{h}{E_0}\sqrt{h^2(h^2+\lambda)^2 - E_0^2}.$$

This equation can be identified with the one obtained from the OC machinery when polar coordinates were used [Eq. (3.3b)], by just replacing $\lambda \to K$, $E_0 \to -d$. Eventually, the geodesic curves obtained in the **h** plane can be parametrized by a Euclidean arc length in order to obtain the actual penetration profile.

D. Numerical integration scheme

The main shortcoming of the methods previously presented for the integration of Hamilton equations is that they rely on knowledge of the constants of motion. In general, the relation of these quantities to the boundary conditions is by no means simple. On the other hand, the practical implications of our model are related to problems in which the field penetration profile must be obtained in terms of the values at the sample's surface $\mathbf{h}(1)$. For instance, such is the case of the magnetic moment of the sample $m[\mathbf{h}(1)]$. For this purpose, we have developed a numerical scheme which allows us to obtain the integral curves of our problem.

On using a Cartesian coordinate system, the optimal control formulation leads to a system of coupled first-order differential equations, which are required to satisfy boundary conditions both at the sample's surface and center. In the partial penetration regime, the simple linear solution requires no effort to be computed. Nevertheless, for the case of full penetration, the method is more involved. We have a two-point boundary value problem for the nonlinear system:

$$\frac{dh_y}{dx} = p_y/\sqrt{p_y^2+p_z^2},$$

$$\frac{dh_z}{dx} = p_z/\sqrt{p_y^2+p_z^2},$$

$$\frac{dp_y}{dx} = 2h_y,$$

$$\frac{dp_z}{dx} = 2h_z, \tag{3.8}$$

with boundary conditions $\mathbf{h}(1) = \mathbf{h}_1$, $h_y(0) = 0$, and $p_z(0) = 0$. In other words, one must solve a system of the kind

$$\mathbf{f}' = \mathbf{g}(\mathbf{f}),$$

where the vector function **f** represents the canonical coordinates $\mathbf{f} \equiv (h_y, h_z, p_y, p_z)$ and **g** is a symbol for Eqs. (3.8). On the other hand, these first-order differential equations are subjected to boundary conditions of the kind $\mathbf{b}[\mathbf{f}(0), \mathbf{f}(1)] = 0$.

An adapted version of the IMSL routine BVPMS has been used by the authors in order to solve this problem. The algorithm is based on a multiple shooting method[16] which starts with a given initial guess $[\mathbf{h}(0), \mathbf{p}(0)]$ and iteratively corrects the initial value set. This is performed by means of Newton's method until $\mathbf{b} = 0$ is satisfied to the desired accuracy. Owing to the nonlinearity of the system, a parametrization of the problem has been necessary in order to attain convergence. We have embedded the system in a one-parameter family

$$\mathbf{F}' = \mathbf{G}(\mathbf{f}, p),$$

with boundary conditions $\mathbf{B}[\mathbf{f}(0), \mathbf{f}(1), p] = 0$, where $p = 0$ gives a linear problem and $p = 1$ returns to the original problem: $\mathbf{G}(\mathbf{f}, 1) = \mathbf{g}(\mathbf{f})$ and $\mathbf{B}[\mathbf{f}(0), \mathbf{f}(1), 1] = \mathbf{b}[\mathbf{f}(0), \mathbf{f}(1)]$. The constants of the motion have provided an extra benefit. In particular, the relation

$$B_i = p b_i + (1-p)[\mathcal{H}(1) - \mathcal{H}(0)]$$

has been successfully implemented in our program.

IV. APPLICATION TO CYLINDRICAL SYMMETRY

This section is devoted to obtain the field penetration profile for the case of cylindrical symmetry. Although more intricate from the mathematical point of view, the experimental circumstance is customary. Assume an isotropic infinite cylinder of radius R to which an external field is applied parallel to the axis. Assume also that a transport current is held along the same axis at the same time (see Fig. 1). The Maxwell equations then read

$$J_\varphi = -\frac{dH_z}{dr},$$

$$J_z = \frac{1}{r}\frac{d}{dr}(rH_\varphi),$$

and the free energy per unit length,

$$\mathcal{G} = \mu_0 \pi \int_{r_c}^{R} (H_z^2 + H_\varphi^2) r\, dr,$$

where r_c stands for the point where the field profile vanishes in the partial penetration regime and equals zero for full penetration. By analogy to the slab, in what follows we normalize the units according to $\rho \equiv r/R$, $\mathbf{h} \equiv \mathbf{H}/H^*$, and $\mathbf{j} \equiv \mathbf{J}/J_c$. On the other hand, using $\mathfrak{H}$ for the applied field and $\mathfrak{I}$ for the current, we define $h_a = \mathfrak{H}/H^*$ and $i = \mathfrak{I}/(\pi R H^*) = (\pi R^2 J_c)$. Now, it seems more convenient to express minimization in terms of the new variables: $x_1 \equiv \rho h_\varphi$ and $x_2 \equiv h_z$. Then, the optimal control Hamiltonian becomes

$$\mathcal{H} = -\left(\frac{x_1^2}{\rho^2} + x_2^2\right)\rho + \mathbf{p}\cdot\dot{\mathbf{x}},$$

where $\dot{\mathbf{x}}$ means $d\mathbf{x}/d\rho$ and the corresponding canonical equations are

$$\frac{dx_1}{d\rho}=\rho/\sqrt{1+(p_2/\rho p_1)^2},$$

$$\frac{dx_2}{d\rho}=1/\sqrt{1+(\rho p_1/p_2)^2},$$

$$\frac{dp_1}{d\rho}=2x_1/\rho,$$

$$\frac{dp_2}{d\rho}=2x_2\rho.$$

On supplying appropriate boundary conditions, the integral curves for these equations can be obtained. We will concentrate on their numerical integration.

For the case of full penetration, the method mimics the procedure which was used in the slab geometry. The boundary conditions read $x_1(1)=i/2$, $x_2(1)=h_a$, $x_1(0)=0$, and $p_2(0)=0$. Again, multiple shooting combined with Newton's method allows us to fulfill the boundary conditions by means of correcting the trial initial values. A parametrization of the problem has also been necessary owing to the nonlinearity of the system.

More interesting is the case for which partial penetration occurs. Unlike the situation in the slab geometry, no trivial solution arises when the boundary conditions $\mathbf{x}(1)=\mathbf{x}_1$, $\mathbf{x}(\rho_c)=0$ are imposed. In particular, this means that ρ_c is an unknown and a new strategy must be designed. We have chosen a linear change of variable, $z=(\rho-\rho_c)/(1-\rho_c)$, which drives the problem to the interval [0,1]. Then, we define the variable $x_3\equiv\rho_c$ and its conjugate momentum p_3, so that the Hamiltonian becomes

$$\mathcal{H}=-\left\{\frac{x_1^2}{[(1-x_3)z+x_3]^2}+x_2^2\right\}\times[(1-x_3)z+x_3](1-x_3)+\mathbf{p}\cdot\mathbf{x}',$$

$\mathbf{x}'$ standing for $d\mathbf{x}/dz$. The canonical equations then read

$$\frac{dx_1}{dz}=\frac{(1-x_3)[(1-x_3)z+x_3]}{\sqrt{1+(p_2/[(1-x_3)z+x_3]p_1)^2}},$$

$$\frac{dx_2}{dz}=\frac{(1-x_3)}{\sqrt{1+([(1-x_3)z+x_3]p_1/p_2)^2}},$$

$$\frac{dx_3}{dz}=0,$$

$$\frac{dp_1}{dz}=2x_1(1-x_3)/[(1-x_3)z+x_3],$$

$$\frac{dp_2}{dz}=2x_2(1-x_3)[(1-x_3)z+x_3],$$

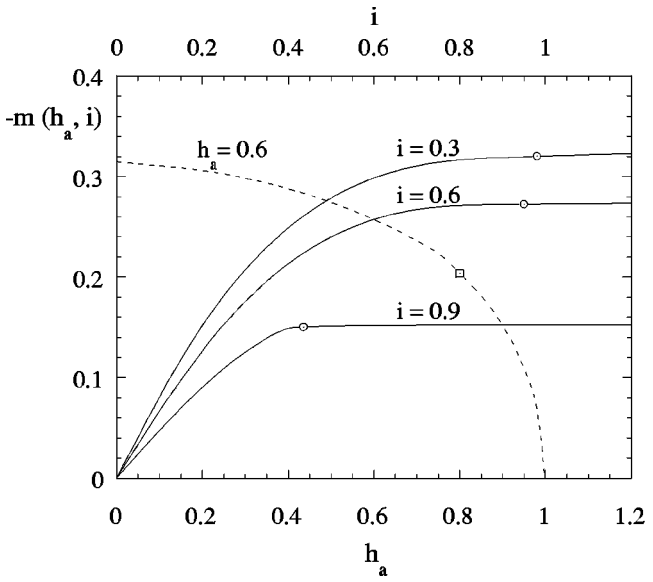

FIG. 4. Predicted behavior for the normalized magnetic moment ($m[\mathbf{h}(1)]=2\int h_z\rho d\rho-h_z(1)$) of a cylindrical superconductor. The applied magnetic field is measured in units of the penetration value H^*, $h_a\equiv\mathfrak{H}/H^*$ and the transport current with respect to the critical density J_c, $i\equiv\mathfrak{I}/(\pi R^2 J_c)$. The solid lines show the evolution of m respect to the applied field for selected values of i, while the dashed curve outlines the reduction of the magnetization for an increasing transport current and fixed h_a. The transition from the partial to the full penetration regime is marked by a symbol over the curves.

$$\frac{dp_3}{dz}=\frac{-x_1^2}{[(1-x_3)z+x_3]^2}+x_2^2\{1-2[(1-x_3)z+x_3]\}-p_1\frac{1-2[(1-x_3)z+x_3]}{\sqrt{1+(p_2/[(1-x_3)z+x_3]p_1)^2}}+\frac{p_2}{\sqrt{1+([(1-x_3)z+x_3]p_1/p_2)^2}}.$$

On the other hand, this system must be integrated subject to

$$x_1(0)=0,\quad x_2(0)=0,\quad p_3(0)=0,$$

$$x_1(1)=i/2,\quad x_2(1)=h_a,\quad p_3(1)=0.$$

Notice that here, x_3 being completely unknown, we have imposed *transversality conditions* by choosing the zero value for the conjugate momentum. Eventually, one can numerically integrate the system. Once more, the multiple shooting method has been used. The algorithm outputs the point $\rho_c=x_3$ and the penetration profile.

This procedure allows us, for instance, to obtain a prediction for the magnetic moment per unit length $m[\mathbf{h}(1)]=2\int h_z\rho d\rho-h_z(1)$. Figure 4 shows this quantity for selected values of $h_z(1)$ and i. Notice the saturation of the magnetic moment m for increasing values of the applied field h_a, as well as the collapse to zero when the transport current i reaches the critical value. Notice also that each curve has been marked with a symbol which indicates the transition from the partial to the full penetration regime. This transition point has been estimated by means of a simplified model which assumes a *single-region uniform current*

distribution.[17] In that model, the relation $h_a^2+i^2=1$ characterizes the external field values for which the sample center is reached. We want to mention that such an approach would be exact for the case of the slab [see Fig. 3(b)] and nearly fits the minimum energy solution for the partially penetrated cylinder. In this work, we have integrated the partial (full) penetration canonical equations, while approaching from below (above) to such point.

V. DISCUSSION AND CONCLUSIONS

We proposed a variational principle which allows us to describe the metastable equilibrium state of flux penetration in a type-II superconductor. The theory developed assumes the simple expression $\mathcal{G}=(\mu_0/2)\int_V \mathbf{H}^2 d^3\mathbf{r}$ for the free energy to be minimized. This is the relevant contribution for field values in the range $H_{c1}\ll H\ll H_{c2}$ where $\mathbf{B}=\mu_0\mathbf{H}$ is also a good approximation for hard superconductors and one can use the picture of pinned nonoverlapping vortices. On the other hand, minimization is carried out under the constraint $|\mathbf{J}|\leqslant J_c$ for the coarse-grained current density. As mentioned before, such a limitation is supported by experimental evidence in the case of high-T_c superconductors.[14]

Our work deals with multicomponent field situations induced by the simultaneous application of a magnetic field $\mathfrak{H}$ and transport current $\mathfrak{I}$. Although we have analyzed both planar (slab) and cylindrical symmetric problems, the main effort of this work is devoted to the former case. In fact, the subsequent discussion refers to that situation. We just want to mention that the qualitative features for the cylinder solution are essentially the same and will be discussed elsewhere.

For sufficiently small values of $\mathfrak{H}$ and $\mathfrak{I}$ the minimum energy is attained in a partial penetration regime, for which the magnetic field vector remains parallel to its value at the surface and its magnitude is progressively reduced, eventually vanishing at some point within the sample. Moreover, the current density vector **J** is constant and perpendicular to **H** everywhere. This can be understood in terms of the relation (valid for the slab geometry)

$$\mathbf{J}=\nabla\times\mathbf{H}=\frac{dH}{dx}\hat{\boldsymbol{\theta}}-H\frac{d\theta}{dx}\hat{\mathbf{H}}=J_\perp\hat{\boldsymbol{\theta}}+J_\parallel\hat{\mathbf{H}}, \qquad (5.1)$$

where θ is the angle between **H** and the y axis (see Fig. 5). Inasmuch as no further restriction that a maximum modulus is imposed, all the current is employed in reducing the magnitude H so that we get $J=J_\perp=J_c$.

On the other hand, for the full penetration regime, field rotation occurs in general, as the magnetic field is an arbitrary vector at the surface and must be directed along the z axis at the center (at least this must happen if one does not accept infinite current densities within the superconductor). By virtue of Eq. (5.1), field rotation is related to the existence of $J_\parallel$. In this case, **J** is no longer a constant vector. *The OC theory permits us to predict the condition* $|\mathbf{J}|=J_c$ *and the distribution rule for the components of* **J**. Figure 5 illustrates the magnetic field reduction and/or rotation towards the center of the sample as well as the angle between the fields for the cases mentioned before.

We want to stress that our particular choice for the space of current densities, i.e., the disk $|\mathbf{J}|\leqslant J_c$, is merely a possible one. Different spaces could be used under the same mathematical treatment, like a rectangular one, $J_\perp\leqslant J_{c\perp}$, $J_\parallel\leqslant J_{c\parallel}$, similar to that proposed by Clem,[11] and a dependence of the critical current densities on the local magnetic field $J_{c\perp}(\mathbf{B})$, $J_{c\parallel}(\mathbf{B})$, even anisotropically, could also be incorporated for a better adjustment to data, without extra conceptual difficulties.

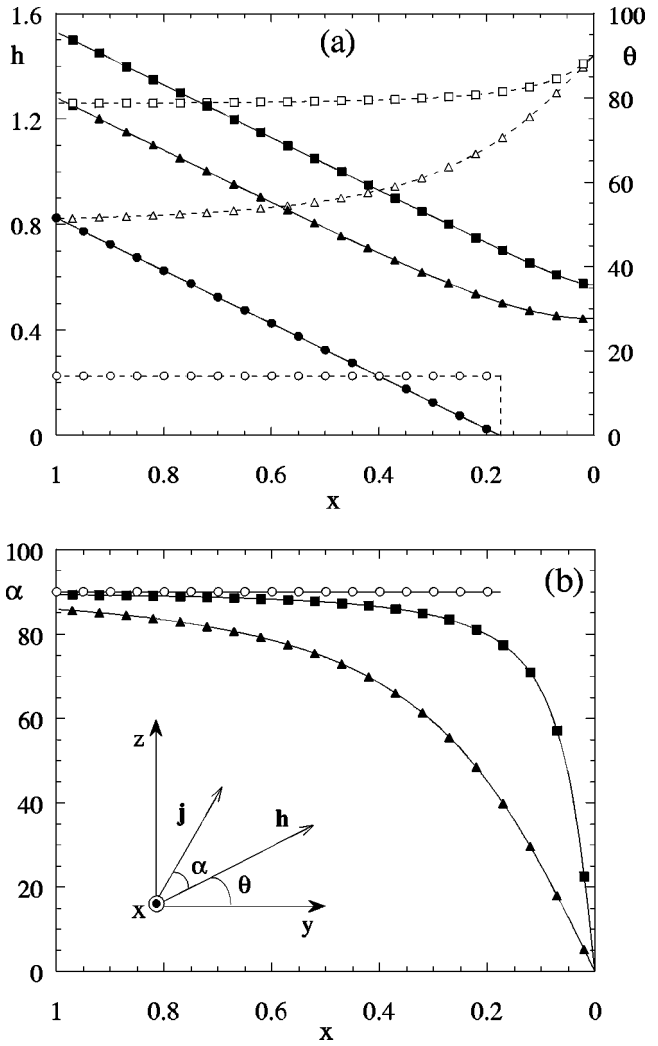

FIG. 5. (a) Field modulus h reduction (solid symbols) and rotation θ (open symbols) vs the penetration coordinate x in a superconducting slab, for several applied values $\mathbf{h}(1)$ at the surface. θ is defined in the inset of panel (b). We have chosen the same external conditions as in Figs. 2 and 3 and again squares stand for $\mathbf{h}(1)=(0.3,1.5)$, triangles for (0.8,1), and circles for (0.8,0.2). In panel (b) we present the rotation angle α between the current vector **j** and the local field **h** for the profiles illustrated in panel (a). The angles are measured in degrees and the rest of the quantities in dimensionless units: $\mathbf{h}\equiv\mathbf{H}/H^*$, $\mathbf{j}\equiv\mathbf{J}/J_c$.

Nevertheless, the simplicity of the control space used in this article brings out the essential physics and allows a wide understanding of the problem. We have obtained analytical expressions for the penetration profile in terms of Weierstrass' elliptic and associated functions. This has been possible by exploiting the *constants of the motion*, whence one can integrate the OC Hamiltonian equations by quadrature. Furthermore, these constants (K,d) allow the classification of the penetration curves in terms of the external field and

current applied values and to present a complete *phase diagram* of the corresponding situations (see Fig. 2).

Simple expressions arise for initial values fulfilling the condition $K=0$. Additionally, and closely related to the analytical solutions, one can formulate the problem in terms of metric spaces. Field penetration can be portrayed as the problem of finding a geodesic in the **h** plane for a particular metric, again defined in terms of (K,d). This provides a pictorial description of the physical phenomenon, which has been mainly a consistency test in the present configuration but which could envisage the properties of the solution for more complex cases.

Moreover, the objective function, the magnetostatic energy density, is also a particular choice suggested by the pinning force balance, but other functions could possibly give different penetration profiles, using the same mathematical tools. For instance, one can use $dg=\mathbf{H}\cdot d\mathbf{B}$ for the free energy density and incorporate the equilibrium response of the vortex assembly $\mathbf{B}(\mathbf{H})$. One could also choose to minimize the penetration depth (for partial penetration) and obtain in this case the same solution profile. On the other hand, it is clear that in order to predict the hysteresis cycle we need to consider a different objective function. The magnetic inertia of the sample, owing to the viscous damping against vortex motion, points towards the use of a function measuring the change of magnetic vector (both in magnitude and direction). At least, this kind of objective function reproduces the simple solution for one-dimensional problems, with a sign change of J beginning at the surface and an unaffected profile in the inner regions of the sample when the magnetic field is cycled.

Additionally, rotating field processes as well as general multicomponent situations would be manageable. Boundary effects produced by the finite size of the sample could also be modeled in this framework by using OC theory for partial differential equations, when the fields depend on more than one coordinate. Stochastic OC theory could be used to represent the complicated distribution of critical current densities in different regions for highly inhomogeneous samples as is the case of high-T_c ceramics. In conclusion, the range of possibilities open to the use of OC theory is wide and can include other physical models where self-organized criticality plays a role, if closed spaces with maximal (critical) values for some variables are used.

ACKNOWLEDGMENTS

The authors want to thank Dr. L. Martín-Moreno for helpful and stimulating discussions at several stages of this work. C.L. acknowledges partial financial support from DGICYT under Project No. DGES-PB96-0717. A.B. and J.L.G. have been supported by CICYT under Project No. MAT95-0921-C02-02.

*Electronic address: anabadia@posta.unizar.es

[1] L. S. Pontryagin, V. Boltyanskiĭ, R. Gramkrelidze, and E. Mischenko, *The Mathematical Theory of Optimal Processes* (Wiley Interscience, New York, 1962).

[2] G. Leitmann, *The Calculus of Variations and Optimal Control*, Mathematical Concepts and Methods in Science and Engineering, Vol. 24, edited by A. Miele (Plenum Press, New York, 1981).

[3] G. Knowles, *An Introduction to Applied Optimal Control* (Academic Press, New York, 1981).

[4] S. Chern, Notices AMS **43**(9), 959 (1996).

[5] P. L. Antonelli and R. Miron, *Lagrangian and Finsler Geometry* (Kluwer, Dordrecht, 1996).

[6] W. Liu and H. J. Sussmann, Mem. Am. Math. Soc. **118** (564), 1 (1995).

[7] A. A. Agrachev and A. V. Sarychev, Ann. Inst. Henri Poincaré Phys. Theor. **13**, 635 (1996).

[8] M. Tinkham, *Introduction to Superconductivity*, 2nd ed. (McGraw-Hill, New York, 1996).

[9] G. Blatter, M. W. Feigel'man, V. B. Geshkenbein, A. I. Larkin, and V. M. Vinokur, Rev. Mod. Phys. **8**, 1125 (1994).

[10] C. P. Bean, Phys. Rev. Lett. **8**, 250 (1962); Rev. Mod. Phys. **36**, 31 (1964).

[11] J. R. Clem, Phys. Rev. B **26**, 2463 (1982).

[12] J. R. Clem and A. Pérez-González, Phys. Rev. B **30**, 5041 (1984).

[13] L. Prigozhin, J. Comput. Phys. **129**, 190 (1996).

[14] G. P. Gordeev, L. A. Akselrod, S. L. Ginzburg, V. N. Zabenkin, and I. M. Lazebnik, Phys. Rev. B **55**, 9025 (1997).

[15] *Handbook of Mathematical Function*, edited by M. Abramowitz and I. A. Stegun (Dover, New York, 1970).

[16] G. Sewell (unpublished).

[17] J. L. Giordano, L. A. Angurel, F. Lera, C. Rillo, and R. Navarro, Physica C **235-240**, 2989 (1994).